This full text paper was peer-reviewed at the direction of IEEE Instrumentation and Measurement Society prior to the acceptance and publication.

Block Based Dense Stereo Matching Using Adaptive Cost Aggregation and Limited Disparity Estimation

Xiao Yang, Xiaobo Chen
State Key Laboratory of Mechanical System and Vibration
Shanghai JiaoTong University
Shanghai, China
yangxiao1992@sjtu.edu.cn

Juntong Xi*
State Key Laboratory of Mechanical System and Vibration
Shanghai JiaoTong University
Shanghai, China

Abstract- Stereo matching is the key problem in many stereo vison based 3D applications. One of the factors make local stereo matching time-consuming is that every pixel has the same disparity range as the pre-set one, which should be larger than all possible disparities. An improper pre-set disparity range may lead to redundant computation for some pixels and inadequate computation for some others. In this paper, we propose an accurate and fast local stereo matching method, which employs fine disparity estimation and adaptive cost aggregation. The main contributions of our work include two parts. Firstly, we use phase-based correlation to estimate an initial disparity range for block center pixels. Secondly, we estimate a more limited disparity range for every in-block pixel according to its support weight to the block center pixel. Our disparity estimation and block matching techniques can not only reduce the disparity searching range for every pixel, but also can eliminate some pseudo match pairs. Four standard Middlebury stereo image pairs are tested to evaluate the performance of the proposed algorithm. Experimental results show that the proposed algorithm can reduce the matching time by 37.4% on average with relatively higher accuracy compared to traditional method.

Keywords—dense stereo matching; block matching; disparity estimation; phase-based correlation

I. INTRODUCTION

Stereo matching is one of the most important branches in both computer vision and machine vision. Applications of stereo matching are active in the fields such as 3D shape measurement[1, 2], vehicle automatic navigation[3], 3D reconstruction[4, 5], and target tracking[6], etc. Problems of low surface texture, repetitive surface texture, and fuzzy color make dense stereo matching always a challenging problem. Beyond that, the amount of computation in stereo matching directly relates to camera resolution, complexity of matching algorithm, and the searching range for exact disparity, etc.

Dense stereo matching algorithms can be classified into local methods and global methods. Global methods[7-9] aim to minimize an optimized energy cost function with every pixel contributing to the one to be matched with a specific weight. Multi-iterations and high resolution of the source image pair make global methods computational-complex and time-consuming. However, global methods are usually more accurate than local ones.

Local methods employ the adjacent pixel-information to find the most similar correspondence in target image for the center pixel in the reference image. The process can be summarized into four steps. Namely, cost computation, cost aggregation, disparity selection and optimization, disparity refinement. To eliminate the edge-blurring problem, almost all recent local matching methods focus on ASW (Adaptive Support Weight) cost aggregation. Bilateral filter[10] and guided filter[11] are two typical edge-preserving filtering methods. Recent stereo matching with ASW can be classified into bilateral weight based methods[12-15] and guided filter weight based methods[16-19], etc. Beyond that, Asmaa et al.[20] first proposed the so-called geodesic support weight basing on the geodesic distance. But the matching accuracy is a little bit worse than bilateral weight and guided filter weight[21]. The generality of these algorithms is that the cost aggregation is regarded as filtering on the cost-volume[16]. In other words, every pixel in the reference image has the same disparity range, which leads to a mass of redundant computation in cost computation step.

In this paper, we propose a new matching strategy that is different from all local stereo matching methods. Firstly, disparity range for block center pixel is estimated by phase-based correlation[22]. Secondly, disparity range for every in-block pixel is limited according to its support weight to the block center pixel. During the process, we adopt ASW, Winner-Takes-All[23], and left-right consistency checking[17] to obtain the initial disparity map. Finally, we adopt weighted median filter[24] to refine the disparity map. Experimental results show that our method can obtain the state-of-art dense disparity map with quite short time.

The remainder of this paper is organized as follows: The proposed disparity range estimation and block matching techniques are introduced in Section II. In Section III, we present the detailed matching process. Some experiment results and discussions are reported in Section IV. Finally, conclusions are drawn in Section V.

Acknowledgement: This work is supported by Scientific Research Project of Shanghai Science and Technology Committee (15111107902 15111102203).

978-1-5090-3596-0/17/$31.00 ©2017 IEEE

II. PROPOSED DISPARITY ESTIMATION STRATEGY

A. Phase-based correlation

For traditional local stereo matching, a three dimensional disparity space image (DSI) is firstly established in the cost computation step. The height of DSI is the maximum disparity for the whole image pair. The length and width of DSI are the number of columns and number of rows, respectively. Therefore, every pixel in the reference image is computed for N times if the maximum disparity is N. For a raw image pair, the maximum disparity is unknown, an improper disparity range may lead to redundant or inadequate cost computation.

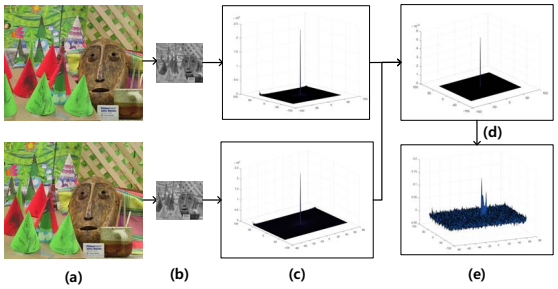

Fig. 1. Phase-based correlation. (a) Raw image pair. (b) Down sampled image pair from (a) with rate ε. (c) Fourier transform of (b). (d) Normalized cross power spectrum of (c). (e) Inverse Fourier transform of (d).

Therefore, phase-based correlation is introduced to estimate a proper disparity range for a raw image pair in following. For a two dimensional image $I_R(x,y)$, its translational transform $I_T(x,y)$ in spatial domain can be expressed as:

$$I_T(x,y) = I_R(x-x_0, y-y_0) \tag{1}$$

Where (x_0, y_0) is the displacement vector in image coordinate. After Fourier transform of the two images, the spatial displacements then correspond to phase differences in the Fourier frequency domain.

$$F_T(u,v) = e^{-i(uu_0+vv_0)} F_R(u,v) \tag{2}$$

Where $F_T(u,v)$ and $F_R(u,v)$ are the Fourier transform of $I_T(x,y)$ and $I_R(x,y)$, repectively. (u_0, v_0) is the corresponding phase shifting vector. Then the normalized cross power spectrum is computed by:

$$P(u,v) = \frac{F_T(u,v) \cdot F_R{}^*(u,v)}{\left|F_T(u,v) \cdot F_R{}^*(u,v)\right|} = e^{-i(uu_0+vv_0)} \tag{3}$$

Where $*$ indicates the complex conjugate. Then doing inverse Fourier transform for $P(u,v)$, a two dimensional Dirichlet function $\delta(x-x_0, y-y_0)$ with peak value $\delta(x_0, y_0)$ can be obtained. Therefore, the peak coordinate (x_0, y_0) indicates the displacements in spatial domain. Fig.1 shows a schematic use of phase-based correlation for raw image disparity range estimation in the proposed algorithm.

B. Block Matching

For a rectified image pair, only horizontal displacements exist in image plane due to epipolar line constraint. One pixel in reference image only need to be matched with someone on the same row in the target image. Fig.2 shows the principle of disparity range estimation for block center matching by phase-based correlation method. Firstly, the reference image is divided into small blocks (e.g. ,pixel size of 11× 11 in Fig.2). By doing phase-based correlation for the raw stereo image pair, an approximate disparity $d_{estimate}$ is acquired. Then, the estimated disparity range ω_{right} for the block center pixel is set by setting two empirical upper bound d_{max} and lower bound d_{min}. Thirdly, the block center is matched within the estimated disparity range. Assuming the in-block pixels have similar disparities to the obtained disparity of the block center, each in-block pixel is furthermore given a more limited disparity range according to its similarity to the center pixel.

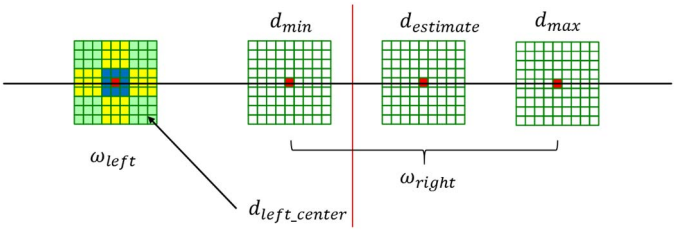

Fig. 2. Block matching with estimated disparity range.

Disparity range estimation method for each in-block pixel is shown in Fig. 3, e.g., setting an empirical step value d_{step}, the half interval value δ_d of the disparity range is a product of some ratio τ and d_{step}. In the proposed algorithm, d_{step} is set to be 6. The in-block disparity range is determined by the following equations:

$$\tau_q = \begin{cases} 1, & w_{pq} > 0.8 \\ 2, & w_{pq} > 0.5 \\ 3, & else \end{cases} \tag{4}$$

$$d_q^{higher} = d_{estimate} + \tau_q * d_{step} \tag{5}$$

$$d_q^{lower} = d_{estimate} - \tau_q * d_{step} \tag{6}$$

Where p denotes the block center pixel, and q denotes the in-block pixel. In equation (4), w_{pq} is ASW coefficient, which is computed by equation (10) in Section III-B. The thresholds for w_{pq} are set by experimental optimization, which do not need to be accurate because they are just set for estimating a more limited disparity range for every in-block pixel. $d_{estimate}$ is the disparity of p, which is achieved by block center matching

introduced above. d_q^{higher} and d_q^{lower} denote the higher bound and lower bound of the limited disparity range of q, respectively. Fig.3(d) shows that the proposed algorithm can limit the disparity range for each in-block pixel effectively, which gives a significant evidence for the effectiveness of the proposed algorithm.

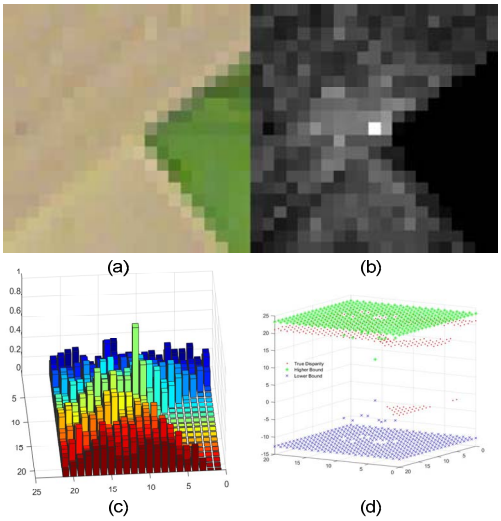

Fig. 3. In-block disparity range estimation. (a) A small block of left image of Cones. (b) Weight coefficients of the block. (c) 3D effect of (b). (d) Limited disparity range of each in-block pixel.

III. Matching Algorithm with Disparity Estimation

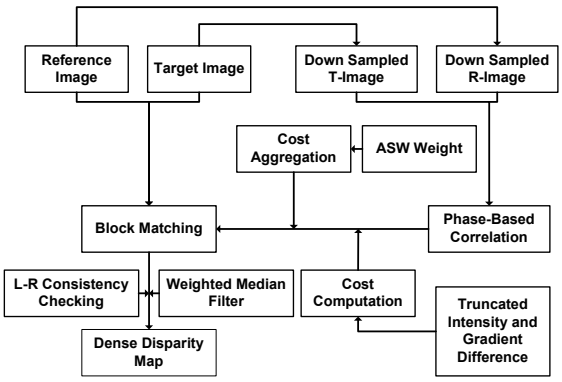

Fig. 4. Schematic process of proposed matching algorithm.

The proposed matching algorithm is an accurate and fast local stereo matching method. In this section, a detailed matching process is presented, which is based on fine disparity range estimation introduced in Section II. An overview of matching process is provided in Fig. 4. Firstly, we do phase-based correlation on a down sampled image pair from the raw stereo image pair. Secondly, we do block matching on the raw stereo image pair.

In details, we first divide the reference image into several individual small blocks. The center of each block is matched with disparity range ω_{right} following the steps of cost computation, ASW cost aggregation, and disparity selection described in below. Then, every in-block pixel of each block is matched with a specifically estimated range computed by equation (5) and (6) following the same steps.

Finally, we use left-right consistency checking to detect the occluded pixels and employ weighted median filter to refine the disparity map.

A. Cost computation

A combined use of truncated intensity difference and truncated gradient difference is robust to photometric distortion[25].

$$C_I(x,y,d) = \min\left\{T_I, \frac{1}{3}\sum_{i=R,G,B}\left|{I_{Ref}}^i(x,y) - {I_{Tar}}^i(x-d,y)\right|\right\} \quad (7)$$

Where Ref and Tar represent the reference image and target image, respectively. d represents a possible disparity value. $C_I(x,y,d)$ is the truncated intensity difference of pixel (x,y) in the reference image with disparity d. T_I denotes the truncation value of intensity difference. ${I_{Ref}}^i$ represents the intensity in the ith channel of the reference image in RGB color space. Similarly, I_{Tar} represents the intensity of the target image.

$$C_{G_i}(x,y,d) = \min\left\{T_{G_i}, \left|G^i_{Ref}(x,y) - G^i_{Tar}(x-d,y)\right|\right\} \quad (8)$$

Where index i denotes x direction or y direction. $C_{G_i}(x,y,d)$ is the truncated gradient difference of pixel (x,y) in the reference image with disparity d. T_{G_i} denotes the truncation value of gradient difference in ith direction. G^i_{Ref} and G^i_{Tar} represent the absolute values of gradient in ith direction of the gray-style reference image and target image, respectively.

$$C(x,y,d) = \alpha C_I(x,y,d) + \beta C_{G_x}(x,y,d) + \gamma C_{G_y}(x,y,d) \quad (9)$$

Where $C(x,y,d)$ is the combined cost of pixel (x,y) with disparity d, which is a weighted summation of absolute intensity difference in RGB color space, absolute gradient differences in x direction and y direction. The weight coefficients for the three parts are α, β, and γ, respectively.

B. ASW Cost Aggregation

As described in Section III-A, the cost of every pixel with an assigned disparity d can be computed. For local stereo matching, every pixel in the small support window is assumed to have the same disparity. To eliminate the problem of edge-blurring due to this assumption. The in-window pixel that has the similar disparity to the center pixel should be given a larger weight coefficient, otherwise should be given a smaller weight

coefficient. In the proposed algorithm, the weight coefficients are computed according to the spatial dissimilarity and intensity dissimilarity in CIE-Lab color space[26]. The gamut of CIE-Lab color space exceeds that of RGB color space. In addition, CIE-Lab model is device independent. Therefore, it is reasonable to assume that the distance in CIE-Lab color space can represent the perceived color difference of two pixels[12].

$$w_{pq} = \exp\left(-\frac{\Delta C_{pq}}{\lambda_C}\right) \cdot \exp\left(-\frac{\Delta D_{pq}}{\lambda_D}\right) \tag{10}$$

$$\Delta C_{pq} = \sqrt{\sum_{i=L,a,b} (I_p{}^i - I_q{}^i)^2} \tag{11}$$

Where ΔC_{pq} represents the Euclidean distance of the colors of center pixel p and adjacent in-window pixel q in Lab color space. ΔD_{pq} represents the spatial Euclidean distance of p and q.

Then, the aggregated correspondence cost for the window center pixel is expressed as:

$$C_p(x, y, d) = \sum_{\substack{x'=p_x-r \\ y'=p_y-r}}^{\substack{x'=p_x+r \\ y'=p_y+r}} w_{pq} \cdot C(x', y', d) \tag{12}$$

Where r is the radius of the support window. p_x and p_y are the x coordinate and y coordinate of p, repectively.

C. Disparity Selection and Occlusion Detection

The lowest aggregated correspondence cost within the estimated disparity range is chosen as the winner cost. The corresponding disparity value is regarded as the true disparity. Left image is first regarded as the reference image to match the right image following the above steps. Then the same procedure is repeated expect for regarding the right image as the reference image to match the left image. Then left-right consistency checking is implemented for the two raw disparity maps to obtain non-occluded disparity map of left image. The disparities of occluded pixels on left disparity map are assigned to zeros.

D. Post Processing for Left Disparity Refinement

The occluded pixels almost correspond to the shaded pixels in the right image. Since pixels of a nearer object to the stereo cameras have larger disparities than a farther one, the occluded pixels on the left disparity map are filled with the lower ones of their horizontal adjacent disparities. Weighted median filter is further used to eliminate the stretching effect caused above. The weight coefficients and the size of filtering kernel here are the same as the ones of ASW setting in the context.

IV. Experiments and Discussion

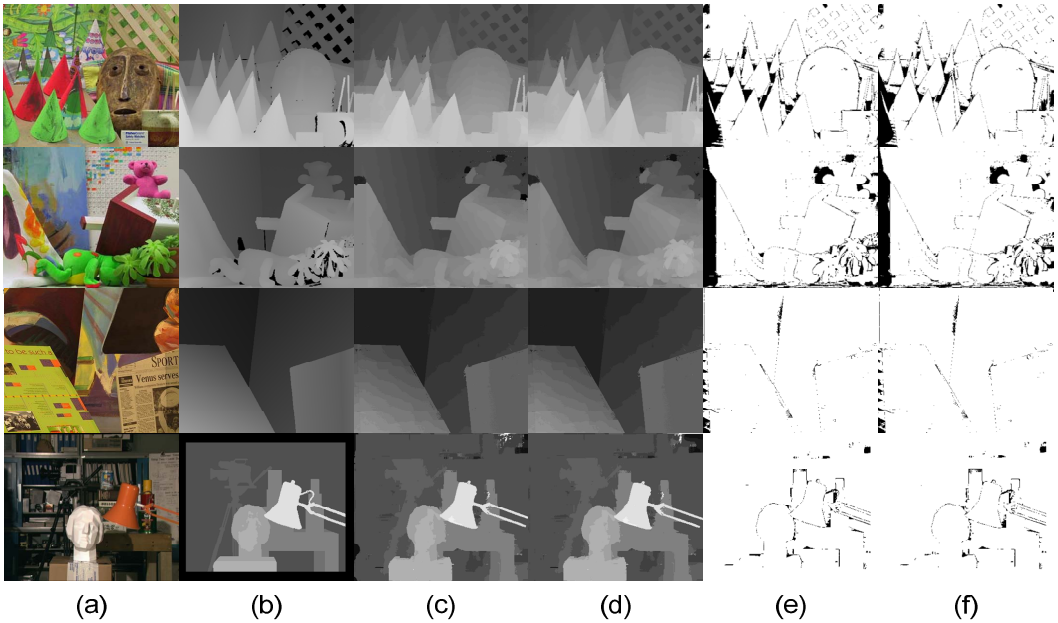

Fig. 5. Experimental disparity maps of Cones, Teddy, Venus, and Tsukuba (From top to bottom). (a) The left image of the four standard image pairs. (b) Ground truths. (c) Raw ASW. (d) Proposed algorithm. (e) Error disparity maps of Raw ASW. (f) Error disparity maps of proposed algorithm.

A. Experiment setup and Evaluation methods

TABLE I. PARAMETER SETTING FOR RAW ASW AND PROPOSED ALGORITHM.

Parameter	ε	ω_{right}	T_I	$T_{G_{x/y}}$	α
Value	3	$2 \times d_{estimate}$	8	7	0.10
Parameter	β	γ	λ_C	λ_D	r
Value	0.55	0.35	9.6	14.14	10/19

We test four standard stereo image pairs from Middlebury Platform[27], i.e., Cones, Teddy, Venus, and Tsukuba, to verify the effectiveness of the proposed algorithm. Two groups of experiments are executed by C++ language on a normal Intel(R) Core(TM) i7-4710MQ CPU 2.50GHz laptop without any acceleration techniques. The only differences of the two groups are the use of the proposed disparity estimation and block matching techniques. We denote the comparative group as Raw ASW Matching in below. Parameters setting for experiments are listed in Table 1. r is set to 19 for Venus, and 10 for others. The other parameters remained the same in two groups. β is set to be larger than γ because the image pairs are in alignment in x direction. α is set to 0.1 to repress image noise. The other parameters are adjusted by experimental optimization with reference to[14, 18].

Both of the matching accuracy and computation time are compared to validate the performance of proposed algorithm. Each experimental disparity map is evaluated in three regions by setting an error threshold 1 compared to the ground truth. The three different regions are namely, non-occluded region (i.e., nooocc), disparity discontinuous region (i.e., disc), and all region for the whole image (i.e., all).

$$\mathrm{E}_{Reg} = \frac{\sum_{(x,y)\in Reg}(\left|d_{ex}(x,y) - d_{gt}(x,y)\right| > 1.0)}{M} \quad (13)$$

Where E_{Reg} denotes the error rate of Reg region. d_{ex} and d_{gt} denote experimental disparity map and the corresponding ground truth, respectively. M denotes the number of pixels in Reg region. Here Reg can be nooocc, dics, or all.

B. *Performance and Discussion*

Experimental results of the two groups are presented in Fig 5. Corresponding accuracy and computation time are shown in Table 2. Experimental results show that the proposed algorithm is superior to Raw ASW both in matching accuracy and matching efficiency. Especially for matching efficiency, the proposed algorithm reduces the average matching time of the four testing image pairs by about 37.4%. This is a universal result for local stereo matching, since almost all the local stereo matching methods follow the same steps as those in Raw ASW. Therefore, the proposed algorithm can be extended to other local stereo matching methods to get improvements in accuracy and matching efficiency.

TABLE II. EVALUATION RESULTS OF MATCHING ACCURACY(ERROR RATE) AND EFFICIENCY(COMPUTATION TIME)

Algorithm		Raw ASW	Proposed
Cones	nooocc	0.02212	**0.02210**
	disc	0.49123	**0.44069**
	all	0.09255	**0.09134**
	time(s)	98.683	**60.332**
Teddy	nooocc	0.05447	**0.05321**
	disc	0.59693	**0.55362**
	all	0.14602	**0.14374**
	time(s)	95.986	**62.694**
Venus	nooocc	0.00544	**0.00548**
	disc	0.21323	**0.16068**
	all	0.01379	**0.01336**
	time(s)	178.456	**107.096**
Tsukuba	nooocc	0.01473	**0.01465**
	disc	0.16992	**0.16239**
	all	0.02379	**0.02314**
	time(s)	21.650	**16.942**
Average	nooocc	0.02419	**0.02386**
	disc	0.36783	**0.32935**
	all	0.06904	**0.06789**
	time(s)	98.694	**61.766**

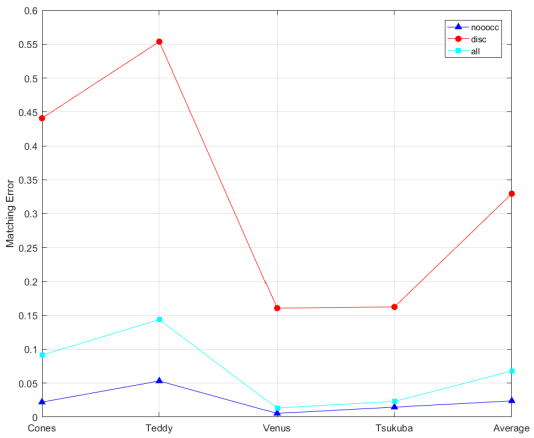

Fig. 6. Error rates of proposed algorithm in three different regions.

There are mainly two contributions of the proposed algorithm. The effects of local stereo matching on texture lacking or periodic texture regions are relatively poor in spite of state-of-art algorithm than that on texture unrepeatable regions. With the help of disparity range estimation by phase-based correlation and the block matching method, some foregoing block center pixels are first matched. Then every in-block pixel is matched within a more limited disparity range, which can restrain the above problem partly. On the other hand, once a reliable disparity of block center pixel is obtained, every in-block pixel gets a specific disparity range. As described in Section III, a higher weight coefficient indicates a more similar disparity to the disparity of the center pixel. In other words, if the weight coefficient of one in-block pixel is much higher, a much more limited disparity range will be assigned to.

Therefore, the amount of computation for every pixel to be matched is reduced.

Furthermore, to give an intuitional evaluation of the accuracy performance, Fig.6 plots the error rates in three different regions. We can see that the matching error in disc regions is comparatively higher than nooocc region. e.g., matching error in disc region is over 10 times than nooocc region for Teddy. While the matching error in disc region does not directly relate to the performance of matching algorithm, which is mainly due to the performance of post processing algorithm. Therefore, the low matching error in nooocc region gives a convincing explanation of the good accuracy performance of the proposed algorithm.

V. CONCLUSION

In this paper, we propose a new local stereo matching method for rectified image pair using adaptive support weight. Main innovation of the proposed stereo matching algorithm is that the disparity range for every pixel is limited due to the fine disparity estimation of the raw image pair and block matching techniques. Phased-based correlation method is used to estimate the disparity range for block center pixels, firstly. Then, the disparity range of every in-block pixel is limited according to the support weight coefficient and the disparity of the matched block center pixel. Experimental results show that the proposed algorithm is superior to the traditional ASW matching method both in accuracy and computation efficiency. It is worth mentioning that the proposed algorithm decreases the average matching time by 37.4% of four standard Middlebury stereo image pairs compared to traditional method.

REFERENCE

[1] S. Zhang, "Recent progresses on real-time 3D shape measurement using digital fringe projection techniques," *Optics & Lasers in Engineering,* vol. 48, pp. 149-158, 2010.

[2] H. Kieu, T. Pan, Z. Wang, M. Le, H. Nguyen, and M. Vo, "Accurate 3D shape measurement of multiple separate objects with stereo vision," *Measurement Science & Technology,* vol. 25, pp. 1-7, 2014.

[3] S. Jiang, Z. Hong, Y. Zhang, and Y. Han, "Automatic path planning and navigation with stereo cameras," in *International Workshop on Earth Observation and Remote Sensing Applications*, 2014, pp. 289-293.

[4] J. K. Suhr, H. G. Jung, K. Bae, and J. Kim, "Automatic free parking space detection by using motion stereo-based 3D reconstruction," *Machine Vision and Applications,* vol. 21, pp. 163-176, 2010.

[5] F. Bruno, G. Bianco, M. Muzzupappa, S. Barone, and A. V. Razionale, "Experimentation of structured light and stereo vision for underwater 3D reconstruction ☆," *Isprs Journal of Photogrammetry & Remote Sensing,* vol. 66, pp. 508-518, 2011.

[6] J. Zhang, L. McMillan, and J. Yu, "Robust Tracking and Stereo Matching under Variable Illumination," 2006, pp. 871-878.

[7] J. C. Kim, K. M. Lee, B. T. Choi, and U. L. Sang, "A Dense Stereo Matching Using Two-Pass Dynamic Programming with Generalized Ground Control Points," *Proceedings / CVPR, IEEE Computer Society Conference on Computer Vision and Pattern Recognition. IEEE Computer Society Conference on Computer Vision and Pattern Recognition,* vol. 2, pp. 1075-1082 vol. 2, 2005.

[8] N. Papadakis and V. Caselles, "Multi-label depth estimation for graph cuts stereo problems," *Journal of Mathematical Imaging and Vision,* vol. 38, pp. 70-82, 2010.

[9] F. Besse, C. Rother, A. Fitzgibbon, and J. Kautz, "PMBP: PatchMatch Belief Propagation for Correspondence Field Estimation," *International Journal of Computer Vision,* vol. 110, pp. 2-13, 2014.

[10] C. Tomasi and R. Manduchi, "Bilateral Filtering for Gray and Color Images," *Iccv,* pp. 839 - 846, 1998.

[11] K. He, J. Sun, and X. Tang, "Guided image filtering," *IEEE Transactions on Software Engineering,* vol. 35, pp. 1397-1409, 2013.

[12] K. J. Yoon and I. S. Kweon, "Locally adaptive support-weight approach for visual correspondence search," in *Computer Vision & Pattern Recognition*, 2005, pp. 924-931.

[13] L. Li, C. M. Zhang, and H. Yan, "Stereo Matching Algorithm Based on a Generalized Bilateral Filter Model," *Journal of Software,* vol. 6, pp. 1906-1913, 2011.

[14] C. H. Lin and C. W. Liu, "Accurate stereo matching algorithm based on cost aggregation with adaptive support weight," *Imaging Science Journal the,* vol. 63, pp. 423-432, 2015.

[15] Y. Zhan, Y. Gu, K. Huang, and C. Zhang, "Accurate Image-guided Stereo Matching with Efficient Matching Cost and Disparity Refinement," *IEEE Transactions on Circuits & Systems for Video Technology,* pp. 1-1, 2015.

[16] Q. Yang, P. Ji, D. Li, S. Yao, and M. Zhang, "Fast stereo matching using adaptive guided filtering ☆," *Image & Vision Computing,* vol. 32, pp. 202-211, 2014.

[17] R. Gao, C. Yun, and L. Yan, "An Improved Stereo Matching Algorithm Based on Guided Image Filter," in *International Conference on Modelling, Identification and Control*, 2015.

[18] A. Hosni, C. Rhemann, M. Bleyer, C. Rother, and M. Gelautz, "Fast cost-volume filtering for visual correspondence and beyond," *IEEE Transactions on Pattern Analysis & Machine Intelligence,* vol. 35, pp. 504-511, 2013.

[19] H. Han, X. Han, and F. Yang, "An improved gradient-based dense stereo correspondence algorithm using guided filter," *Optik - International Journal for Light and Electron Optics,* vol. 125, pp. 115-120, 2014.

[20] A. Hosni, M. Bleyer, M. Gelautz, and C. Rhemann, "Local stereo matching using geodesic support weights," in *IEEE International Conference on Image Processing*, 2009, pp. 2093-2096.

[21] A. Hosni, M. Bleyer, and M. Gelautz, "Secrets of adaptive support weight techniques for local stereo matching ☆," *Computer Vision & Image Understanding,* vol. 117, pp. 620-632, 2013.

[22] Y. Chen, "A windowed phase correlation algorithm for subpixel motion estimation," *Proc Spie,* vol. 7850, pp. 2280-2283, 2010.

[23] D. Scharstein and R. Szeliski, "A Taxonomy and Evaluation of Dense Two-Frame Stereo Correspondence Algorithms," *International Journal of Computer Vision,* vol. 47, pp. 7-42, 2002.

[24] Z. Ma, K. He, Y. Wei, and J. Sun, "Constant Time Weighted Median Filtering for Stereo Matching and Beyond," 2013, pp. 49-56.

[25] G. Gimel'Farb, J. Liu, J. Morris, and P. Delmas, "Concurrent Stereo under Photometric Image Distortions," vol. 1, pp. 111-114, 2006.

[26] X. Zhang and B. A. Wandell, "A spatial extension of CIELAB for digital color-image reproduction," *Journal of the Society for Information Display,* vol. 5, pp. 61–63, 1998.

[27] B. D. Scharstein and R. Szeliski, "Middlebury stereo vision. http://vision.middlebury.edu/stereo," 2010.